Barker, P.F., Camerlenghi, A., Acton, G.D., and Ramsay, A.T.S. (Eds.)
Proceedings of the Ocean Drilling Program, Scientific Results Volume 178

16. Data Report: Seismic Velocity Analysis on the Continental Shelf Transect, ODP Leg 178, Antarctic Peninsula[1]

U. Tinivella,[2] A. Camerlenghi,[2] and M. Rebesco[2]

ABSTRACT

Five analyses of seismic velocity employing acoustic tomography were conducted across the location of the sites proposed for Ocean Drilling Program (ODP) drilling on the continental shelf of the Pacific margin of the Antarctic Peninsula. The resulting interval velocities were supplied to the ODP Site Survey Panel before drilling and are now presented in light of the results of ODP Leg 178 drilling, during which three of the five proposed sites were drilled, as a tie between traveltimes and depths at all sites, and as a tool to aid genetic interpretation of seismic units in future studies. We present details of the methodology, the five stack sections across each site, and the picked horizons used for the velocity analysis. The results of the analysis are presented as interval tomographic velocity sections on a depth scale. Finally, we compare tomographic and stacking velocity profiles for each site location. We summarize the main features of the velocity fields obtained in this study in a short concluding section.

OBJECTIVE

This report provides seismic velocity information that was generated specifically to respond to comments of the Ocean Drilling Program (ODP) Site Survey Panel on the data set provided by proponents of ODP drilling Proposal 452, which proposed drilling the Pacific margin of the

[1]Tinivella, U., Camerlenghi, A., and Rebesco, M., 2001. Data report: Seismic velocity analysis on the continental shelf transect, ODP Leg 178, Antarctic Peninsula. *In* Barker, P.F., Camerlenghi, A., Acton, G.D., and Ramsay, A.T.S. (Eds.), *Proc. ODP, Sci. Results,* 178, 1–25 [Online]. Available from World Wide Web: <http://www-odp.tamu.edu/publications/178_SR/VOLUME/CHAPTERS/SR178_016.PDF>. [Cited YYYY-MM-DD]
[2]Instituto Nazionale di Oceanografia e di Geofisica Sperimentale–OGS, Borgo Grotta Gigante, 42/c I-34010 Sgonico (Trieste), Italy. Correspondence author: **utinivella@ogs.trieste.it**

Initial receipt: 24 January 2001
Acceptance: 1 June 2001
Web publication: 29 August 2001
Ms 178SR-231

Antarctic Peninsula. The velocity analyses were submitted to the ODP Site Survey Data Bank in 1996. Because of the importance of velocity information to the interpretation of the Leg 178 drilling results and, in general, to drilling results on glacial margins, we have assembled the data for publication in the Leg 178 *Scientific Results* volume in the form of a data report so that the results of this analytical study may become more widely available. The information presented refers to five locations on the Leg 178 outer continental shelf transect (Shipboard Scientific Party, 1999a) (Figs. F1, F2).

METHODS

Stacking velocity information (interval velocity derived using Dix's formula from the root-mean-square [RMS] velocity) is the prime seismic velocity information obtainable from a multichannel seismic reflection (MCS) survey. However, although stacking velocities are useful in data processing (they allow correct stack and enable data migration), their use as interval velocities to predict the subbottom depth of a target reflector is, in general, not recommended, especially if the available offset is short compared to the depth of the target. In addition, semblance-velocity analyses and constant-velocity-stack analyses imply that a gross spatial average (the acquisition spread) is applied to the velocity estimation and that a very simple earth model (i.e., homogeneous horizontal layers) is assumed.

In order to obtain additional and independent velocity information and to compare it to the stacking velocities, we have adopted reflection tomography as described in detail by Carrion et al. (1993a, 1993b). We briefly recall its basic concepts below.

The space is discretized by long pixels, which are zones where the propagation velocity of seismic waves is assumed to be constant. The pixel shape may be irregular, and the lateral boundaries are vertical straight lines; the upper and lower boundaries coincide with the interpreted reflecting interfaces (see Böhm et al., 1999). The pixel shape is dictated by the available resolution with a surface acquisition geometry (Böhm et al., 2000) that allows good estimation of the lateral gradients but is poor for the vertical variations between two reflectors. A vertically averaged velocity is estimated between the upper and lower reflector.

Traveltimes are picked manually or in semiautomatic mode (Tinivella, 1998) along selected horizons on common-offset and common-shot gathers. An iterative inversion procedure is started with any initial model, even very far from the true solution. Rays are traced according to Fermat's principle (Vesnaver 1994, 1996a, 1996b) to simulate the seismic wave propagation in that velocity field and reflector position. Data inversion is completed according to the simultaneous iterative reconstruction technique (SIRT) (Van der Sluis and Van der Vorst, 1987; Stewart, 1991). At each step, the velocity distribution is updated first, obtaining an estimate of the depth location of the reflection point for each source-receiver position and for each considered reflector. Then, observing the pattern and the dispersion of these reflection points, a new reflector geometry and local velocity structure are introduced, while also considering lateral velocity gradients. The final solution is obtained by alternately iterating these two steps until a minimum dispersion is obtained for all reflectors. An example of a final solution is presented in Figure F3 (from analysis near the location of Site 1103).

F1. Location map of Leg 178 drill sites, p. 10.

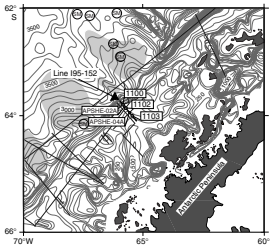

F2. Seismic profile and location of proposed drill sites and actual sites, p. 11.

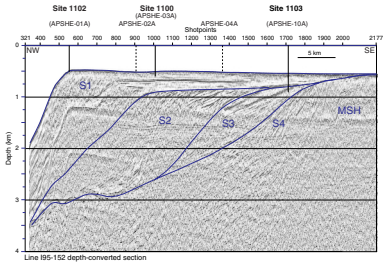

F3. Example of solution of tomographic inversion on picked traveltimes, p. 12.

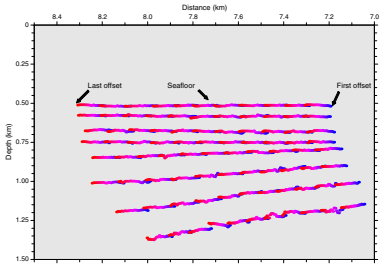

RESOLUTION

Conventional stacking velocity analysis is able to estimate the RMS velocity with sufficient accuracy (2%–3%) if the layers are nearly horizontal and if the incidence angles are small. In this case, we can simply apply Dix's formula to get the interval velocities, which is the information we need to identify anomalous variations of the wave velocity.

Although the accuracy of stacking velocity is sufficient, the space and time resolution of the velocity spectra may be quite limited. In stacking velocity analysis, a spatial average is carried out over the acquisition spread, whose length in our case is 750 m (half of the streamer length). Consequently, we are not able to measure directly sharp lateral velocity variations. Along the time dimension, the coherency values are usually averaged within time windows whose length is comparable to that of the seismic wavelets. Seismic wavelets are band-limited signals; therefore, their direct comparison by semblance or cross-correlation carried out in stacking velocity analysis necessarily provides a band-limited estimate.

Tomographic inversion of traveltimes is able to improve the resolution significantly for two main reasons:

1. The picking procedure transforms seismic reflections into punctual events; although the picking is a spiking process, which concentrates an event into a single point, the picking accuracy is limited by noise presence, interference with other events, phase rotations at supercritical incidence angles, and so on. Therefore, we have to consider this point in a statistical sense, which means that averaging is still necessary for our velocity estimate.
2. There is no spatial average because each event preserves its individual contribution to the velocity estimation during the whole inversion procedure. We can say that the nominal spatial resolution is on the order of the trace spacing, which is 12.5 m in our case. The actual spatial resolution, however, is affected by the size of the Fresnel zone, whose radius is on the order of 60 m at the seafloor with the dominant frequency of 100 Hz.

SEISMIC DATA

Multichannel seismic profile I95-152 was acquired by Programma Nazionale di Ricerche in Antartide (PNRA) in 1995 as part of a program that included the seismic site survey of drill sites proposed to ODP within drilling Proposal 452. The data are described and displayed in Shipboard Scientific Party (1999b, table 19). We list the acquisition parameters in Table T1.

RESULTS

Picking and Inversion

The five parts of the stack section analyzed are illustrated in Figure F4. We have picked seven to nine reflectors with spacing of about 100 ms or less (Fig. F5). Purposely, we did not pick reflectors too close to the seafloor reflector in order to avoid the interference of bubble-induced ringing or streamer ghosts. The picking of reflectors was particularly

T1. Multichannel seismic profile, p. 23.

F4. Variable-density stack sections with approximately no vertical exaggeration across site locations, p. 13.

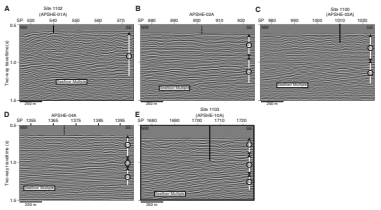

F5. Picked reflections on common-offset gathers, p. 14.

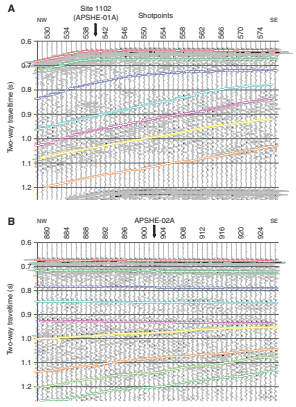

easy in the topsets of Unit S1. In the foresets of Unit S2 and in deeper dipping reflectors of Units S3 and S4, the coherency of reflections is rather weak. The coherency of the reflectors was found to be highest, particularly in common-offset gathers, in traces from 10 to 29 (offsets from 329.5 to 567 m), and these traces have been selected for picking on common-trace and common-offset gathers.

The tomographic inversion has been applied to one of every four shots. As expected, the coherency of the inversion of the traveltimes is weaker in foreset reflectors (e.g., see Fig. F3), but it has always been possible to obtain a satisfactory final solution for all picked reflectors. The uncertainty in the velocity estimation with this method is typically a few percent. Although we have no estimates of the uncertainty in this application, a ±2% error was estimated in a recent application of this method by us in an area with generally poorer reflector continuity on the nearby South Shetland margin (Tinivella et al., 1998, fig. 8).

Continental Shelf Edge: Proposed Site APSHE-01A, Drilled as Site 1102

The two-dimensional (2-D) velocity structure across the location of Site 1102 is illustrated in Figure F6A. All reflectors picked are within Unit S1. The shelf break occurs at shotpoint (SP) 538, about 130 m seaward of the site location. The upper part is divided into two topset layers of moderately increasing velocity with depth. Weak lateral velocity changes that do not suggest significant trends are present in these upper layers. Within the third interval, the transition from topset reflectors in the southeast to foreset reflectors in the northwest occurs. A sharp lateral velocity change within this interval, from 1.8 to 2.7 km/s, with increasing velocity toward the northwest, is coincident with such a transition. All underlying intervals are composed of foreset reflectors. Weak lateral velocity changes that do not suggest significant trends are also present in these lower layers. A sharp velocity increase from 1.8 to 3 km/s occurs to the southeast of the site location, between the topset reflectors of the third interval and the foreset reflectors. This coincides with the presence of foreset reflector terminations against the topset reflectors.

A comparison between the tomographic velocity profile at the location of the site and the nearest available stacking velocity profile (SP 575, 875 m southeast of the site location) is illustrated in Figure F7A.

Outer Continental Shelf: Proposed Site APSHE-02A

The 2-D velocity structure across the location of proposed Site APSHE-02A is illustrated in Figure F6B. The topsets of Unit S1 are divided into four layers of increasing velocity with depth. A sharp velocity increase occurs between the first and the second layer of the topset unit. Weak lateral velocity changes that do not suggest significant trends are present in this unit. The velocity increases from about 1.6 to 2.7 km/s in the upper 350 m of sediment. In foresets of Unit S2, the velocity increases from 2.8 to 3.3 km/s. A sharp velocity increase occurs between the lower boundary of the topsets and the upper boundary of the foresets at the southeast end of the analyzed section. This coincides with foreset reflector terminations against the topset reflectors. Northwest of the site, the velocity across the topset/foreset boundary does not increase sharply. A sharp lateral velocity gradient, with increasing ve-

F6. Final solution of the velocity fields, p. 17.

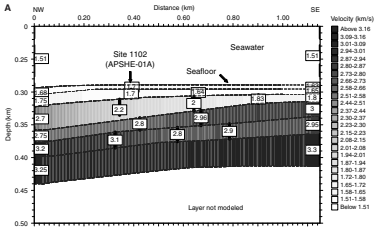

F7. Comparison of tomographic velocity on site and nearest stacking velocity, p. 22.

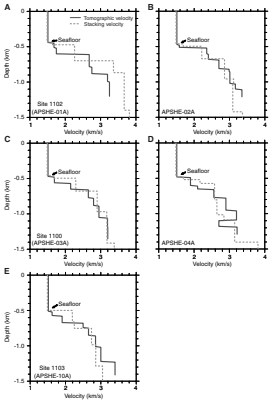

locity to the southeast, is present within the second interval of the foresets of Unit S2.

A comparison between the tomographic velocity profile at the proposed site location and the nearest available stacking velocity profile (SP 895, 175 m northwest of the site location) is illustrated in Figure F7B.

Outer Continental Shelf: Proposed Site APSHE-03A, Drilled as Site 1100

The 2-D velocity structure across the location of proposed Site APSHE-03A is illustrated in Figure F6C. Unit S1 is divided into four layers of increasing velocity with depth. Weak lateral velocity changes are present. The velocity increases from about 1.7 to 2.7 km/s in the upper 400 m of sediment. In the foresets of Unit S2, the velocity increases from 2.95 to 3.3 km/s. Qualitatively, the differences in the velocity distribution between topsets and foresets found at this site location are similar to those described above for the location of proposed Site APSHE-02A location, including lateral gradients within foresets.

Figure F7C illustrates the comparison between tomographic and stacking velocity 700 m southeast of the site location (SP 975).

Outer Continental Shelf: Proposed Site APSHE-04A

The 2-D velocity structure across the location of proposed Site APSHE-04 is illustrated in Figure F6D. The topsets of Unit S1 are divided into three layers of increasing velocity with depth. Lateral velocity changes are present in this unit: in the first layer an increase occurs from the southeast end of the analyzed section toward the northwest; in the third layer, an even sharper increase occurs from the northwest end of the analyzed section toward the site, and hence, gradually decreases. Within this unit, the velocity increases from ~1.7 to ~2.7 km/s in the upper 300 m of sediment. Unit S2 is divided into two layers of increasing velocity with depth. Also, at this location, velocity increases sharply at the boundary between topsets and foresets. An exception is found directly northwest of the site location, where the velocity across the topset/foreset boundary does not increase sharply because of the relatively high velocity in the topset layer. A velocity decrease (velocity inversion) occurs at the boundary between glacial reflectors of Unit S2 to "early glacial or non-glacial" reflectors of Unit S3. Within S3, the velocity increases from 2.8 to about 3.5 km/s. A lateral gradient is present in the lowest layer, with a decrease toward the outer shelf (northwest).

See Figure F7D for a comparison between the tomographic velocity at the site location and the nearest available stacking velocity profile (SP 1375, 125 m southeast of the site location).

Outer Continental Shelf: Proposed Site APSHE-10A, Drilled as Site 1103

The 2-D velocity structure across the Site 1103 location is illustrated in Figure F6E. The topsets of Unit S1 are divided into three layers of increasing velocity with depth. The velocity increases from about 1.6 to 2.5 km/s in the upper 250 m of sediment. Unit S2 is missing at this location. Within Unit S3, the velocity increases from 2.7 to 3.0 km/s. The sharp velocity increase below the lower boundary of Unit S1 found at

all other outer shelf sites is not present here. The velocity increases more gradually throughout and lateral gradients are present only in the second layer of Unit S1, with an increase toward the inner shelf (southeast). The only sharp increase downward is between Units S3 and S4 (from 3 to 3.4–3.5 km/s).

See Figure F7E for a comparison between the tomographic velocity profile at the site location and the nearest available stacking velocity profile (SP 1695, 300 m northeast of the site location).

Time-Depth Relations

According to the velocity fields presented, we have identified the time-depth relationships for the seafloor, the bottoms of the drilled holes at the three drilled sites, and the S1/S3 boundary at Site 1103 (Table T2).

T2. Time-depth correlation, p. 24.

CONCLUSIONS

We summarize the principal aspects of our analytical work as follows (see [N1]):

1. In the five seismic sections analyzed, we found a generally very steep vertical velocity gradient. The steepest average gradient is found at the continental shelf edge (see Figure F6A at southeast end of the section, including the Site 1102 location) where a velocity of 3 km/s is found at less than 200 m sub-bottom depth. Anomalously high seismic velocity is a common feature in continental shelf sediments of Cenozoic glacial margins, as a consequence of ice load and/or glacial erosion (i.e., Solheim et al., 1991).
2. However, we have not found anomalously high velocity at the seafloor, as may have been expected. For comparison, Cochrane and Cooper (1991) report a velocity of 2.08 m/s at the seafloor at Site 472 (ODP Leg 119 in Prydz Bay), a location geometrically analogous to our Site 1100, and a velocity of 2.4 m/s at the seafloor at other locations on the outer and inner shelf.
3. The sharpest velocity increase downwards is found at the boundary between topsets (above) and foresets (below). One partial exception to this is the Site 1103 location, where such an increase does exist, although it is less than another increase found deeper, between Units S3 and S4.
4. The only sharp velocity inversion occurs at the near-conformable boundary between Units S2 and S3 at proposed Site APSHE-04A.
5. We encountered difficulty in picking coherent reflections in foresets of Unit S1 at Site 1102 and in foresets of Unit S2 at Site 1100. This is due to the poor lateral continuity of reflectors with respect to the topset units, as a consequence of the difference in depositional environments between continental slope and continental shelf, respectively.
6. The comparison between the tomographic and stacking velocity profiles shows that the tomographic velocity is generally lower than the stacking velocity in the upper few hundreds of meters, while significant but variable differences occur below. As

expected, the tomographic velocities provide a higher-resolution, smoother profile than the stacking velocities.

ACKNOWLEDGMENTS

We thank A. Vesnaver and G. Böhm for providing access to and assistance with the tomographic inversion software. C. Pelos and L. Sormani contributed by processing MCS profile I95-152. This research has been funded by Programma Nazionale per le Ricerche in Antartide (PNRA).

REFERENCES

Bart, P.J., and Anderson, J.B., 1995. Seismic record of glacial events affecting the Pacific margin of the northwestern Antarctic Peninsula. *In* Cooper, A.K., Barker, P.F., and Brancolini, G. (Eds.), *Geology and Seismic Stratigraphy of the Antarctic Margin*. Am. Geophys. Union, Antarct. Res. Ser., 68:75–96.

Böhm, G., Galuppo, P., and Vesnaver, A., 2000. 3-D adaptive tomography by Delaunay triangles and Voronoi polygons, *Geophs. Prosp.*, 42:723-744.

Böhm, G., Rossi, G. and Vesnaver, A., 1999. Minimum-time ray-tracing for 3-D irregular grids, *J. Seismic,* 8:117–131.

Camerlenghi, A., Rebesco, M., DeSantis, L., Volpi, V., in press. The Antarctic Peninsula Pacific Margin: modelling flexure and decompaction with constraints from ODP Leg 178 initial results. *N. Z. J. Geol. Geophys*.

Carrion, P., Boehm, G., Marchetti, A., Pettenati, F., and Vesnaver, A., 1993a. Reconstruction of lateral gradients from reflection tomography. *J. Seismic Expl.,* 5:55–67.

Carrion, P., Vesnaver, A., Boehm, G., and Pettenati, F., 1993b. Aperture compensation tomography. *Geophys. Prospect.,* 41:367–380.

Cochrane, G.R., and Cooper, A.K., 1991. Sonobuoy seismic studies at ODP drill sites in Prydz Bay, Antarctica. *In* Barron, J., Larsen, B., et al., *Proc. ODP, Sci. Results,* 119: College Station, TX (Ocean Drilling Program), 27–44.

Larter, R.D., and Barker, P.F., 1991. Neogene interaction of tectonic and glacial processes at the Pacific margin of the Antarctic Peninsula. *In* Macdonald, D.I.M. (Ed.), *Sedimentation, Tectonics and Eustasy: Sea-level Changes at Active Margins*. Spec. Publ. Int. Assoc. Sedimentol., 12:165–186.

Larter, R.D., Rebesco, M., Vanneste, L.E., Gamboa, P.A.P., and Barker, P.F., 1997. Cenozoic tectonic, sedimentary and glacial history of the continental shelf west of Graham Land, Antarctic Peninsula. *In* Barker, P.F., and Cooper, A.K. (Eds.), *Geology and Seismic Stratigraphy of the Antarctic Margin,* Part 2. Am. Geophys. Union Antarctic Research Series, 71:1–27.

Rebesco, M., Camerlenghi, A., and Zanolla, C., 1998. Bathymetry and morphogenesis of the continental margin west of the Antarctic Peninsula. *Terra Antart.,* 5:715–728.

Shipboard Scientific Party, 1999a. Shelf Transect (Sites 1100, 1102, and 1103). *In* Barker, P.F., Camerlenghi, A., Acton, G.D., et al., *Proc. ODP, Init. Repts.,* 178: College Station, TX (Ocean Drilling Program), 1–58.

————, 1999b. Explanatory notes. *In* Barker, P.F., Camerlenghi, A., Acton, G.D., et al., *Proc. ODP, Init. Repts.,* 178, 1–66 [CD-ROM]. Available from: Ocean Drilling Program, Texas A&M University, College Station, TX 77845-9547, U.S.A.

Solheim, A., Forsberg, C.F., and Pittinger, A., 1991. Stepwise consolidation of glacigenic sediments related to the glacial history of Prydz Bay. *In* Barron, J., Larsen, B., et al., *Proc. ODP, Sci. Results,* 119: College Station, TX (Ocean Drilling Program), 169–182.

Stewart, R.R., 1991. Exploration seismic tomography: Fundamentals, *Soc. Explor. Geophys., Course Note Ser.,* 3.

Tinivella, U., 1998. Semi-automatic picking in real seismic data. *First Break,* 16:47–51.

Tinivella, U., Lodolo, E., Camerlenghi, A., and Boehm, G., 1998. Seismic tomography study of a bottom simulating reflector off the South Shetland Islands (Antarctica). *In* Henriet, J.-P., and Mienert, J., (Eds.) *Gas Hydrates: Relevance to World Margin Stability and Climate Change*. Geol. Soc. London, Spec. Publ., 137:141–151.

Van der Sluis, A., and Van der Vorst, H.A., 1987. Numerical solutions of large, sparse linear systems arising from tomographic problems. *In* Nolet, G. (Ed.): *Seismic tomography:* D. Reidel Pub., Dordrecht, Holland, 49–84.

Vesnaver, A., 1994. Towards the uniqueness of tomographic inversion solutions, *J. Seism. Explor.,* 3:323–334.

————, 1996a. Irregular grids in seismic tomography and minimum time ray-tracing, *Geophys. J. Int.,* 125:641–165.
————, 1996b. Ray-tracing based on Fermat's principle in irregular grids, *Geophys. Prospect.,* 44:741–760.

Figure F1. Location map of Leg 178 drill sites along the continental shelf transect. Sites originally selected as drilling targets are labeled as APSHE-01A (drilled as Site 1102), APSHE-02A, APSHE-03A (drilled as Site 1100), APSHE-04A, and APSHE-10A (drilled as Site 1103), according to the labeling in the drilling proposal. Only three of these targets were drilled during Leg 178, as shown in the figure (see also Figure F2, p. 11). Bathymetry is after Rebesco et al. (1998). The location of Istituto Nazionale di Oceanografia e di Geofisica Sperimentale (OGS) multichannel seismic profiles is outlined by black straight lines. The shaded patches on the continental rise outline the inferred extent of sediment drifts.

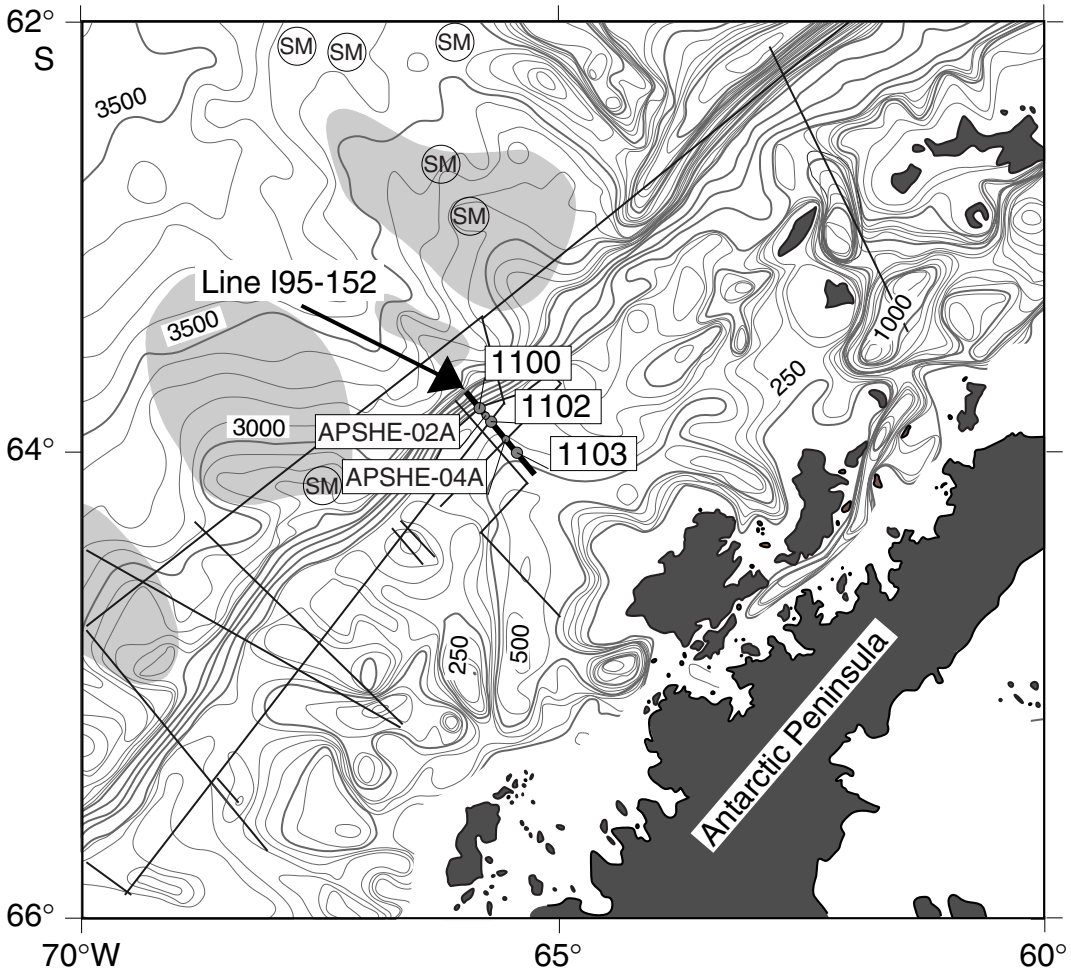

Figure F2. Seismic profile of line I95-152 and location of proposed drill sites and actual sites drilled during Leg 178 for which the velocity analysis has been undertaken (modified after Camerlenghi et al., in press). Location shown in Figure F1, p. 10. MSH = mid-shelf high (Larter and Barker, 1991, Bart and Anderson, 1995). Seismic unit names were adopted during Leg 178 after Larter et al. (1997).

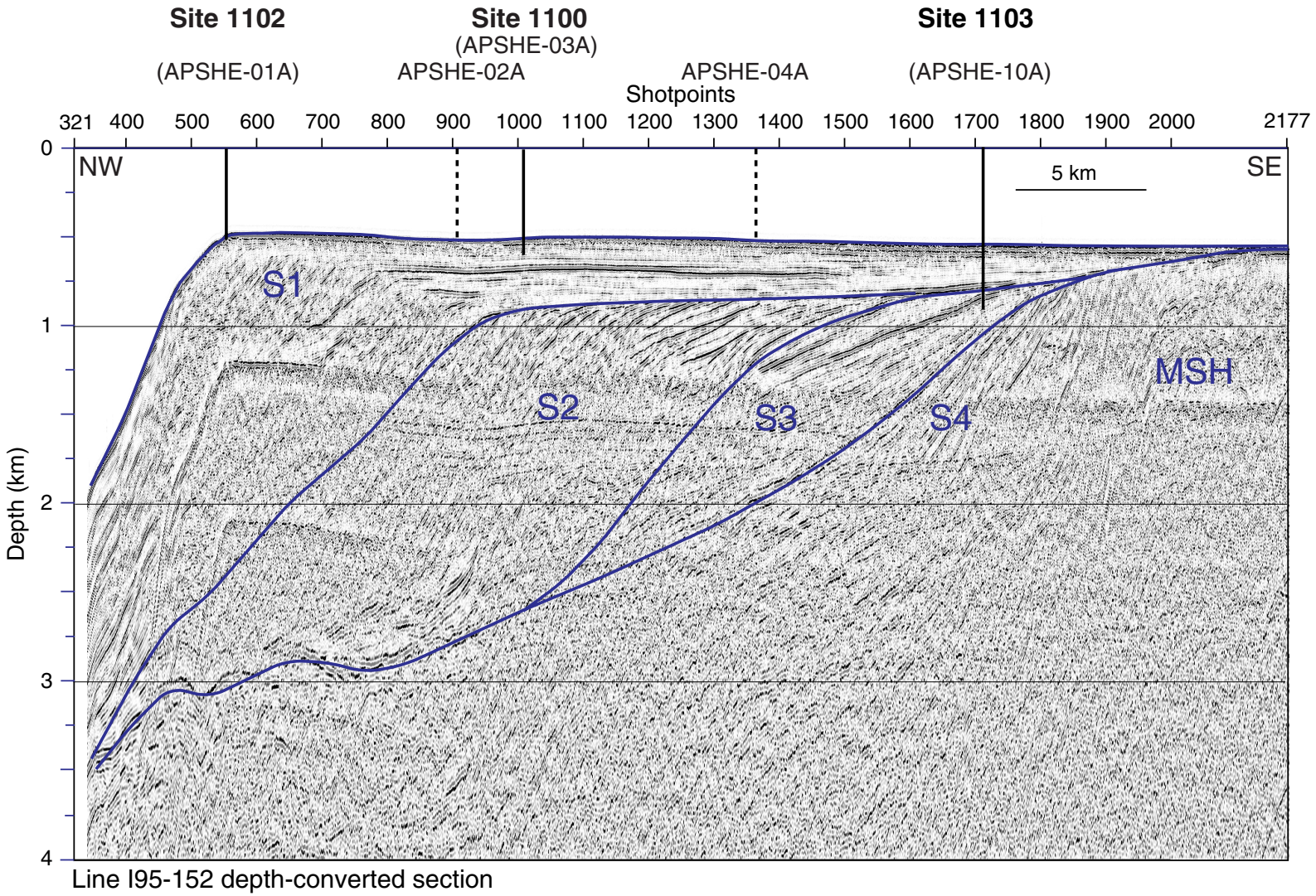

Figure F3. Example of solution of tomographic inversion on picked traveltimes (from the analysis of line I95-152 at Site 1103). In each group of reflection points, changing from blue (darker) to purple (lighter) indicates the picked offsets of one shot. Note the poorer coherency of the reflection points in the lower reflector, belonging to the foresets of seismic Unit S2.

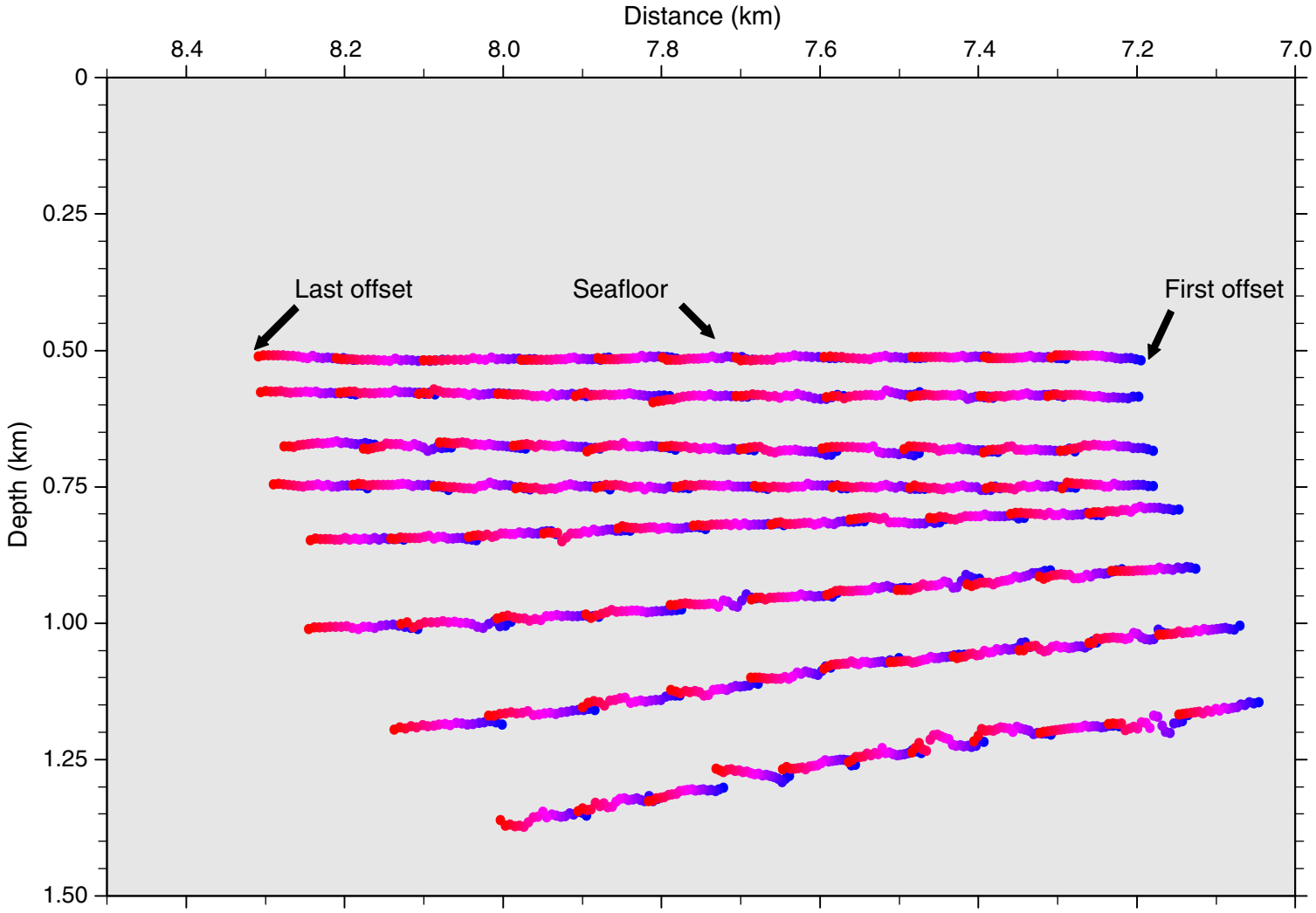

Figure F4. Variable-density stack sections with approximately no vertical exaggeration across proposed and drilled site locations. **A.** Proposed Site APSHE-01A, drilled as Site 1102. The whole section lies within the foresets of Unit S1. **B.** Proposed Site APSHE-02A. Topsets of Unit S1 unconformably overlie foresets of Unit S2. **C.** Proposed Site APSHE-03A, drilled as Site 1100. Topsets of Unit S1 overlie foresets of Unit S2. **D.** Proposed Site APSHE-04A. Conformable succession of Unit S1 topsets, Unit S2 foresets, and subparallel reflectors of Unit S3. **E.** Proposed Site APSHE-10A, drilled as Site 1103. Topsets of Unit S1 overlie Unit S3 near-conformably. The S3/S4 boundary is unconformable. Unit S2 is missing at this location. SP = shotpoint. TWT = two-way traveltime.

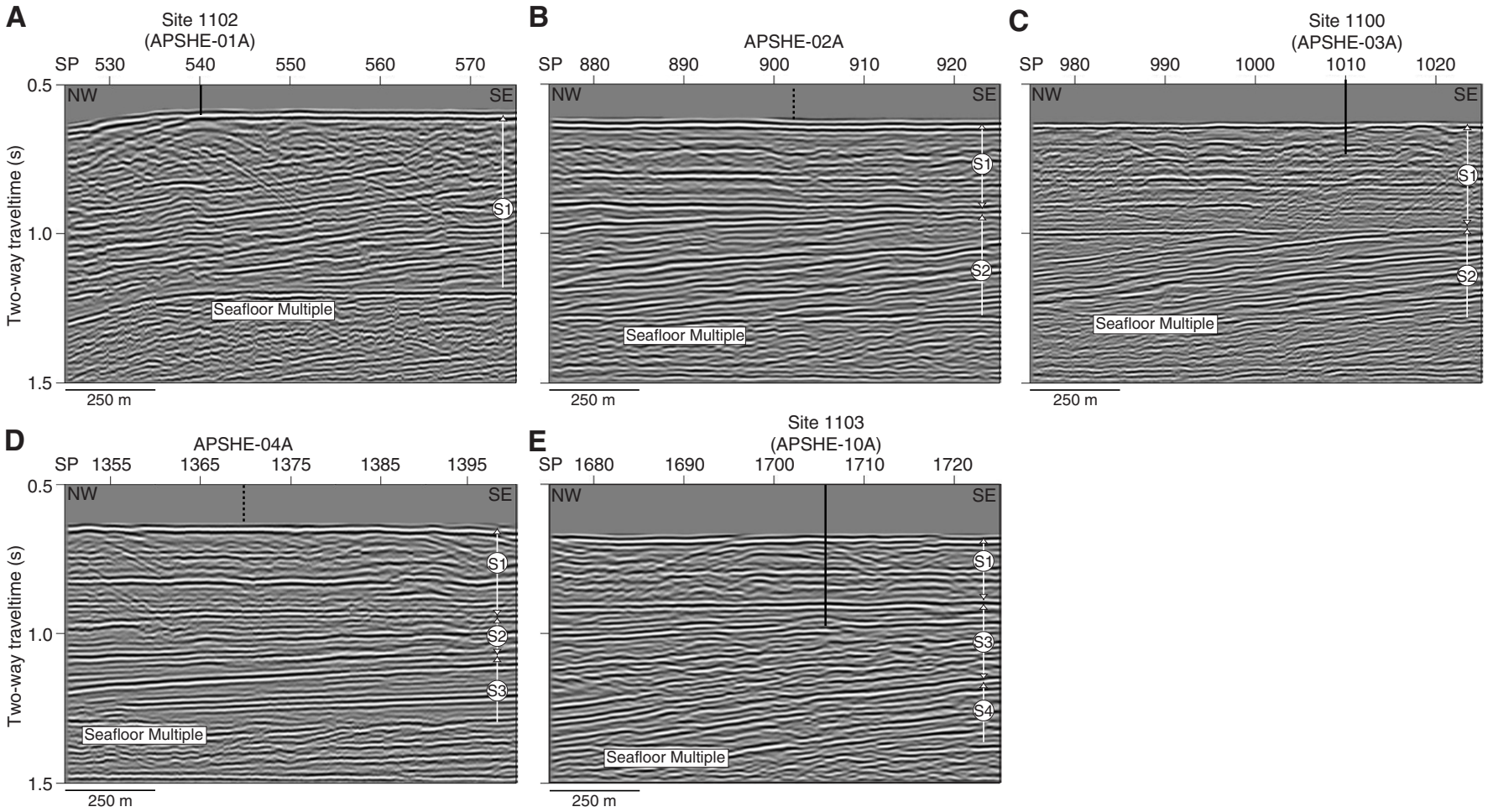

Figure F5. Picked reflections on common-offset gathers. In all cases, we display trace 10, corresponding to 329.5-m offset. See text for comments. **A.** Proposed Site APSHE-01A, drilled as Site 1102. **B.** Proposed Site APSHE-02A. (Continued on next two pages.)

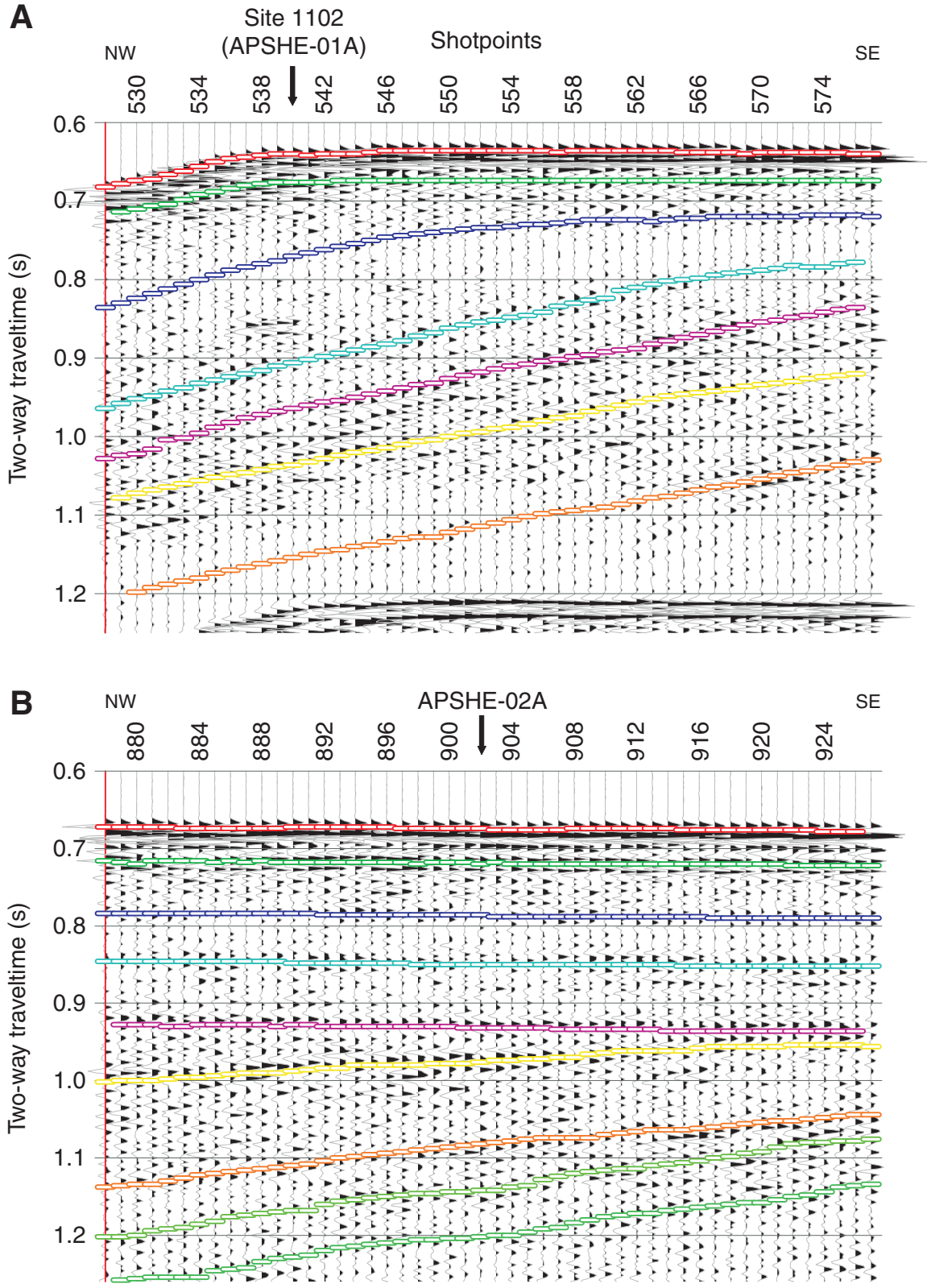

Figure F5 (continued). C. Proposed Site APSHE-03A, drilled as Site 1000. D. Proposed Site APSHE-04A.

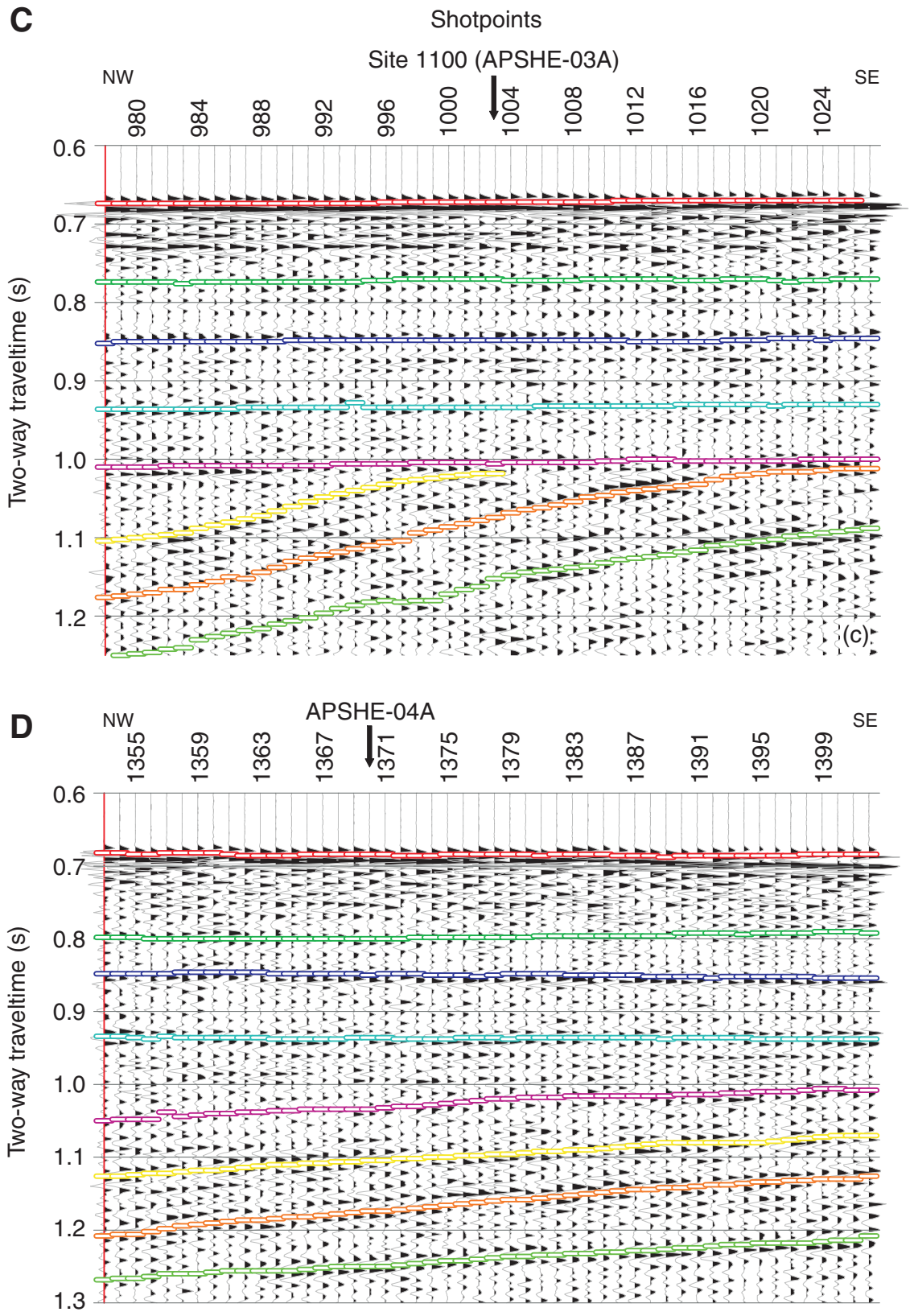

Figure F5 (continued). E. Proposed site APSHE-10A, drilled as Site 1103.

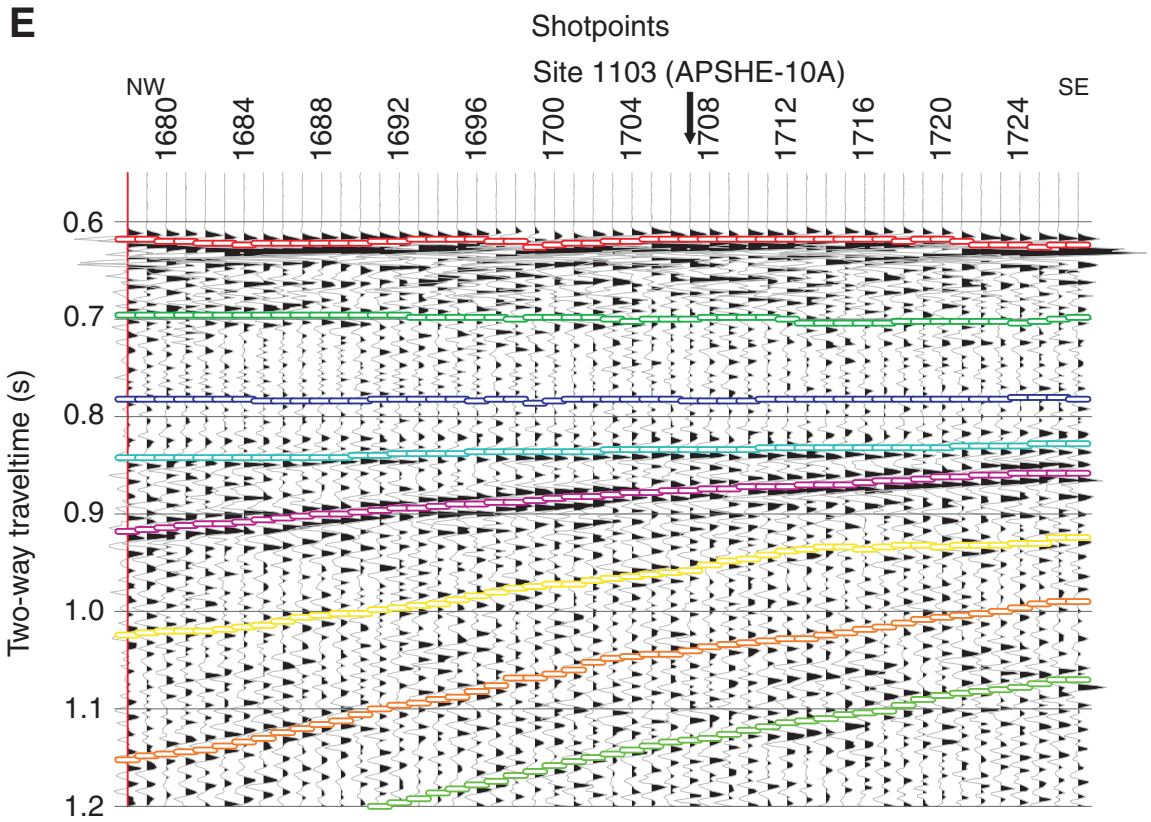

Figure F6. Final solution of the velocity fields. Velocity is indicated in the boxes in kilometers per second. Linear extrapolation is assumed between velocity bars within the same interval. **A.** Proposed Site APSHE-01A, drilled as Site 1102. (Continued on next four pages.)

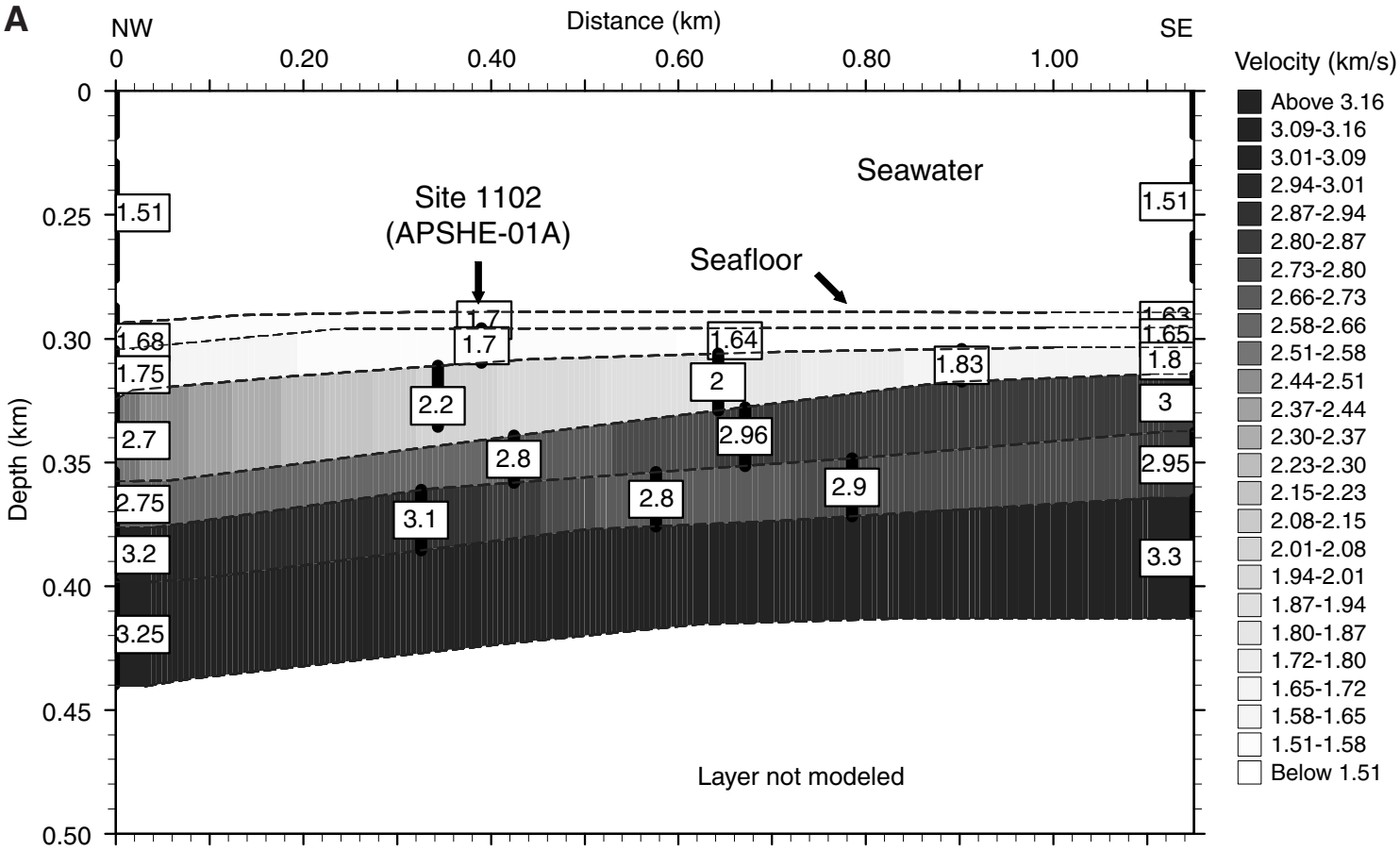

Figure F6. (continued). B. Proposed Site APSHE-02A.

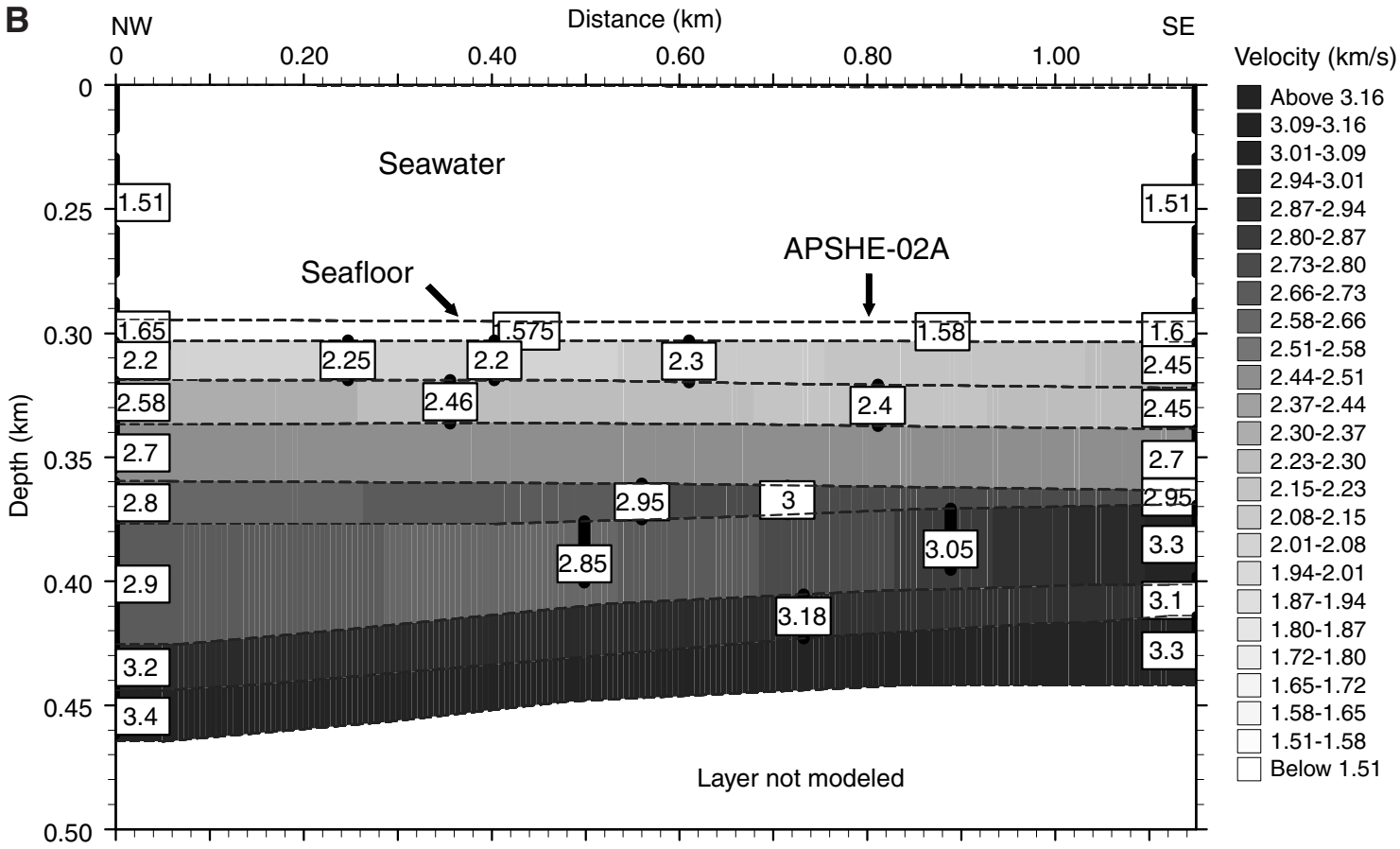

Figure F6. (continued). C. Proposed Site APSHE-03A, drilled as Site 1100.

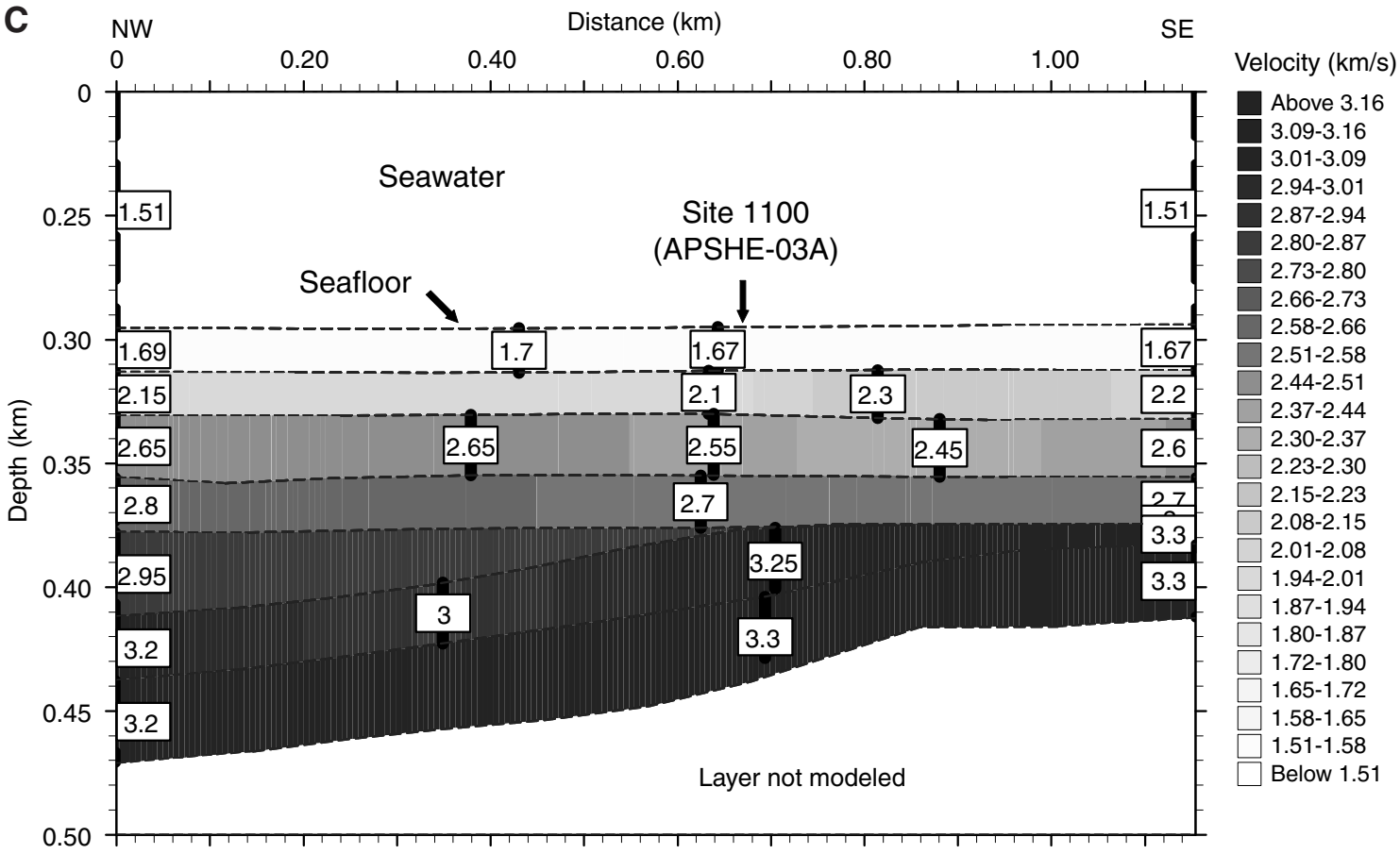

Figure F6. (continued). D. Proposed Site APSHE-04A.

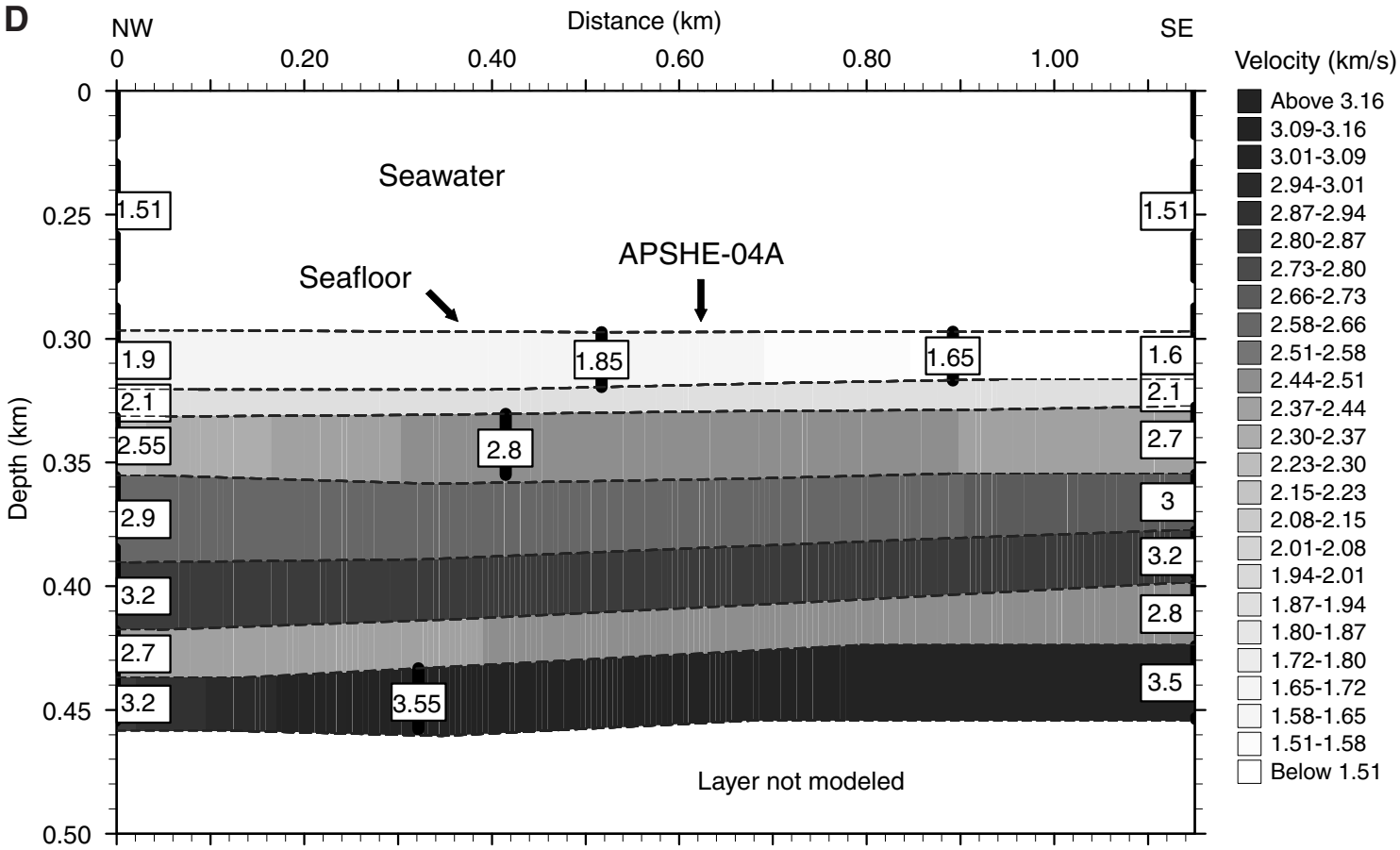

Figure F6. (continued). E. Proposed Site APSHE-10A, drilled as Site 1103.

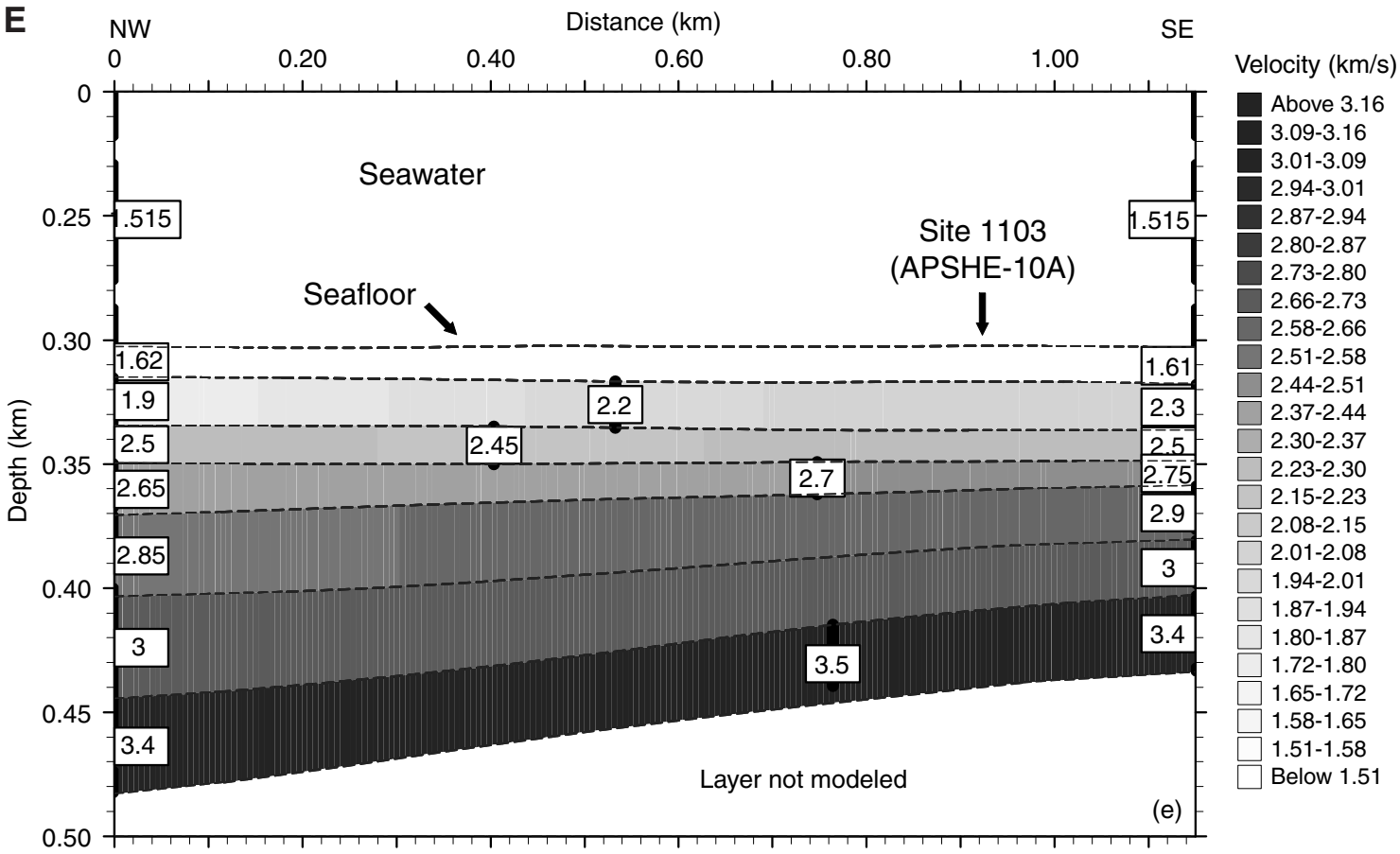

Figure F7. Comparison between tomographic velocity on site and nearest available stacking velocity. See text for comments. **A.** Proposed Site APSHE-01A, drilled as Site 1102. **B.** Proposed Site APSHE-02A. **C.** Proposed Site APSHE-03A, drilled as Site 1100. **D.** Proposed Site APSHE-04A. **E.** Proposed Site APSHE-10A, drilled as Site 1103.

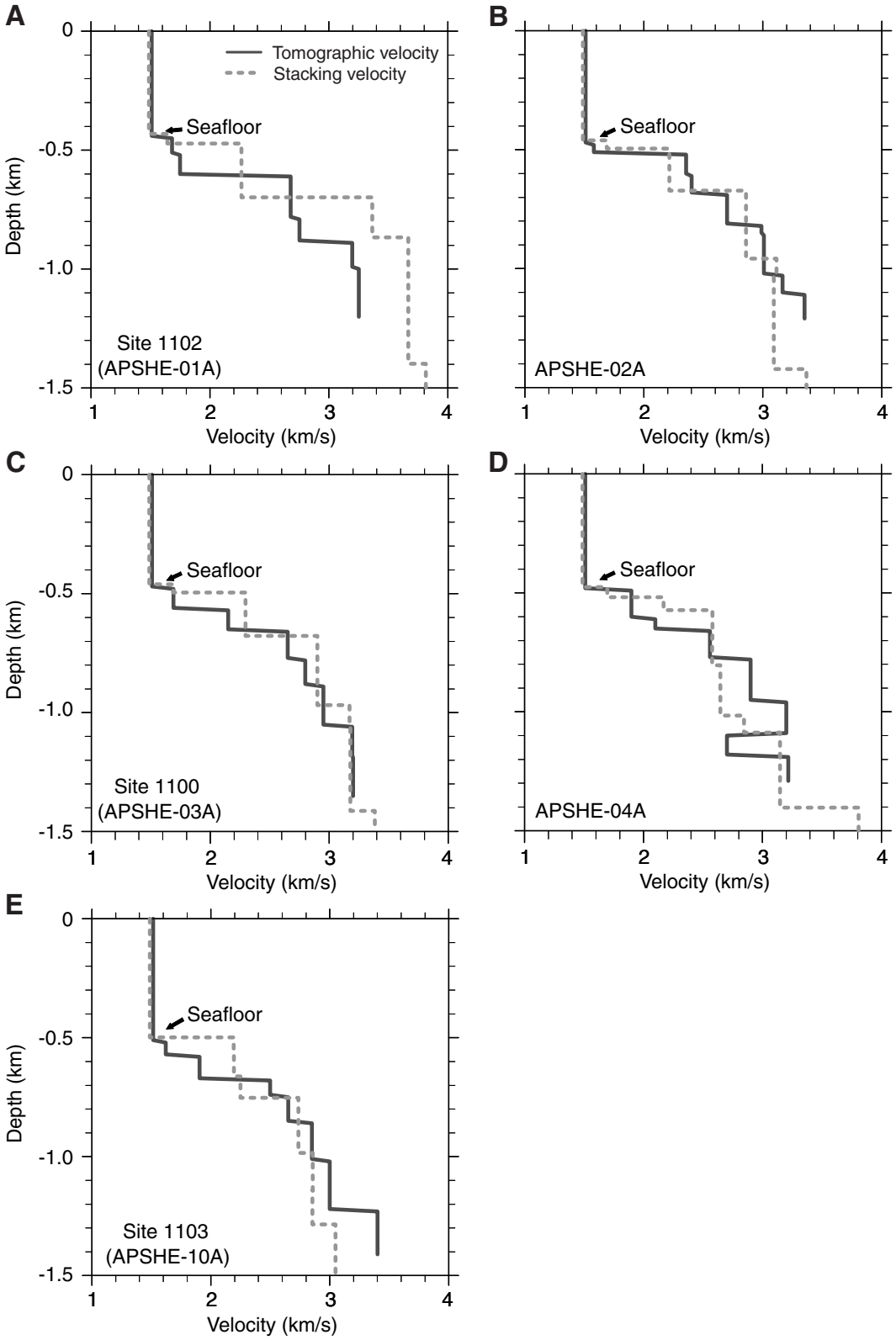

Table T1. Multichannel seismic profile I95-152, acquisition parameters.

Source	
Gun types:	GI
Number of guns:	2
Total volume (in^3):	420
Tow depth (m):	4
Shot interval (m):	25
Sensors	
Number of traces:	120
Length of streamer (m):	1500
Trace interval (m):	12.5
Tow depth (m):	8
Offset of near trace (m):	217
Recording	
Sampling rate (ms):	2
Record length (s):	4
Coverage:	30
Magnetic support:	Tape

Note: GI = generator-injector gun type (by Seismic Systems, Inc.).

Table T2. Time-depth correlation at Sites 1100, 1102, 1103.

	TWT from sea surface (ms)	TWT from seafloor (ms)	Depth from sea surface (m)	Depth from seafloor (mbsf)
Site 1100				
Seafloor	623	0	470.0	0
Bottom of Hole 1100D	750	127	580.5	110.5
Site 1102				
Seafloor	585	0	442.0	0
Bottom of Hole 1102D	602	17	456.9	14.9
Site 1103				
Seafloor	667	0	505.0	0
S1/S3	848	181	742.5	237.5
Bottom of Hole 1103A	985	318	867.7	362.7

Note: TWT = two-way traveltime.

CHAPTER NOTE*

N1. 1 June 2001—Author note: Moerz et al. (in press, this volume) present a velocity analysis at the Site 1103 location that is based on sonic logging. The seismic velocity analyses presented in this report and in that of Moerz and co-authors have a degree of overlap that is not discussed in either paper. We suggest that the interested reader take into consideration both papers for a complete understanding of the velocity structure at Site 1103.

30 January 2002: Moerz et al. (**Chap. 19,** this volume) was published on 28 November 2001.

*Dates reflect file corrections or revisions.